

# Complete history of the observable 21-cm signal from the first stars during the pre-reionization era

Anastasia Fialkov<sup>1\*</sup>, Rennan Barkana<sup>1</sup>, Arazi Pinhas<sup>2</sup>, Eli Visbal<sup>3,4</sup>

<sup>1</sup> *Raymond and Beverly Sackler School of Physics and Astronomy, Tel Aviv University, Tel Aviv 69978, Israel*

<sup>2</sup> *Department of Physics and Astronomy, University of Pennsylvania, 209 South 33rd Street, Philadelphia, PA 19104-6396, USA*

<sup>3</sup> *Jefferson Laboratory of Physics, Harvard University, Cambridge, MA 02138, USA*

<sup>4</sup> *Institute for Theory & Computation, Harvard University, 60 Garden Street, Cambridge, MA 02138, USA*

27 February 2024

## ABSTRACT

We present the first complete calculation of the history of the inhomogeneous 21-cm signal from neutral hydrogen during the era of the first stars. We use hybrid computational methods to capture the large-scale distribution of the first stars, whose radiation couples to the neutral hydrogen emission, and to evaluate the 21-cm signal from  $z \sim 15 - 35$ . In our realistic picture large-scale fluctuations in the 21-cm signal are sourced by the inhomogeneous density field and by the Ly $\alpha$  and X-ray radiative backgrounds. The star formation is suppressed by two spatially varying effects: negative feedback provided by the Lyman-Werner radiative background, and supersonic relative velocities between the gas and dark matter. Our conclusions are quite promising: we find that the fluctuations imprinted by the inhomogeneous Ly $\alpha$  background in the 21-cm signal at  $z \sim 25$  should be detectable with the Square Kilometer Array.

**Key words:** galaxies: formation — galaxies: high redshift — intergalactic medium — cosmology: theory

## 1 INTRODUCTION

The history of the Universe between hydrogen recombination and the end of the epoch of reionization remains mostly unobserved (Barkana & Loeb 2001). Luckily, this era can be probed by measuring the redshifted 21-cm emission of neutral hydrogen. The state of the art radio experiments (e.g., the Murchison Widefield Array (MWA) (Bowman et al. 2009) and the LOw Frequency ARray (LO-FAR) (Harker et al. 2010)) are designed to constrain the 21-cm signal from the epoch of reionization, probing the redshift range  $z \sim 7 - 15$ ; whereas next generation experiments, such as the Square Kilometer Array (SKA) (Carilli et al. 2004), will probe the epoch of primordial star formation out to  $z \sim 30$ .

Prior to reionization, radiation emitted by the first galaxies drove a chain of significant cosmic transitions, which are important to test observationally. In particular, the X-ray background heated the gas above the Cosmic Microwave Background (CMB) temperature; Ly $\alpha$  photons coupled the 21-cm spin temperature to the gas kinetic temperature through the Wouthuysen-Field effect (Wouthuysen 1952; Field 1958), thus making the epoch of primordial star formation available for observations; and, finally, photons in

the Lyman-Werner (LW) band dissociated molecular hydrogen. The relative importance of the three radiative backgrounds is studied in this Letter.

The first stars are believed to form via the cooling of molecular hydrogen (the lowest temperature coolant in the metal-free early Universe), in halos of mass above the threshold minimum cooling mass  $M_{\text{cool}} \sim 10^5 M_{\odot}$  (Tegmark et al. 1997). It is possible, however, that H<sub>2</sub> cooling leads to very inefficient star formation, in which case stars would only form via cooling of atomic hydrogen in more massive halos of  $M_{\text{cool}} \sim 10^7 M_{\odot}$ . According to the common picture of hierarchical structure formation, in which small objects form first, all these halos are expected to be rare (and highly clustered) at high redshift, as they can form only in high density peaks of matter fluctuations (Barkana & Loeb 2004). The rarity is even more extreme due to two effects, which are usually omitted but which we include here. First is the effect of the LW background, which destroys molecular hydrogen and increases the minimum cooling mass, thus acting as negative feedback and delaying star formation. Unfortunately, modeling of this effect in simulations is rather limited at the moment. In fact, the effect of the feedback on  $M_{\text{cool}}$  has been studied only in an unrealistic setup in which the LW intensity during the entire process of gravitational collapse of a halo is fixed (Machacek et al. 2001; Wise & Abel 2007; O’Shea & Norman 2008). Since in reality the LW intensity

\* E-mail: anastasia.fialkov@gmail.com

risers exponentially fast with time (Holzbauer & Furlanetto 2011), there is some uncertainty in how to normalize to the simulation results. In Fialkov et al. (2013) we dealt with this by parameterizing the strength of the feedback and comparing the effect of totally negligible, inefficient (“weak”) and highly efficient (“strong”) LW feedbacks, as well as the case of completely saturated feedback (i.e., no H<sub>2</sub> cooling, when stars are formed only via cooling of atomic hydrogen).

The second important process that we include is the effect of high-redshift inhomogeneous supersonic relative velocities between the baryons and the cold dark matter, denoted by  $v_{bc}$ , on primordial star formation, which only recently was noticed by Tseliakhovich & Hirata (2010). The authors of this paper showed that relative velocities were coherent on scales of several Mpc and their power spectrum exhibited strong Baryon Acoustic Oscillations (BAOs; see also Dalal et al. (2010)). The effect of  $v_{bc}$  on star formation at high redshifts can be dramatic: the coherent stream of baryons through a dark matter halo hinders accretion and redistributes the gas density within the halo. As a result, a heavier halo is needed to form a dense cloud of gas that will allow star formation (Greif et al. 2011; Stacy et al. 2011). Thus, in regions where  $v_{bc}$  is high  $M_{cool}$  is boosted, which delays star formation and increases galaxy clustering (Tseliakhovich et al. 2011; Fialkov et al. 2011).

Unfortunately, the strong fluctuations on large scales in the number of stars, modified by the LW and  $v_{bc}$  effects (Fialkov et al. 2013), make it difficult to predict the 21-cm signal from the epoch of primordial star formation. Visbal et al. (2012) and Fialkov et al. (2013) used a hybrid numerical method (for a detailed discussion of the structure of our simulation see section S1 of the Supplementary Information of the former paper, and references within) to show that the signal from  $z \sim 20$  exhibits strong heating fluctuations on  $\sim 100$  Mpc scales, which can be detected using present day observational technology.

In this Letter we extend the work of Fialkov et al. (2013) by adding a self-consistent inhomogeneous Ly $\alpha$  background, which allows us to compile a more complete history of the 21-cm signal from high redshifts ( $10 \lesssim z \lesssim 40$ ). We use the hybrid methods to evolve in the same framework the large-scale distribution of stars and the three radiative backgrounds emitted by these stars (including Ly $\alpha$ , LW and X-rays and neglecting the ionizing radiation which becomes important at lower redshifts), and to estimate the 21-cm signal from  $10 \lesssim z \lesssim 40$ . We use the standard set of cosmological parameters (Komatsu et al. 2010), a star formation efficiency of  $f_* = 10\%$  (with additional  $\log(M)$  suppression at small masses (Machacek et al. 2001)), LW parameters as explained in detail in Fialkov et al. (2013), and Ly $\alpha$  parameters as in Barkana & Loeb (2005). We assume that the X-ray luminosity is characterized by a power law with a spectral index  $\alpha = 1.5$  and an X-ray photon efficiency of  $\xi_X = 10^{57} M_\odot^{-1}$  as in Mesinger et al. (2011), based on observed starbursts at low redshift. In addition, we account approximately for the redistribution of the UV photons due to their scattering in the wings of the Ly $\alpha$  line of hydrogen (Naoz & Barkana 2008) and for the  $v_{bc}$ -dependent suppression of the filtering mass (Naoz et al. 2013).

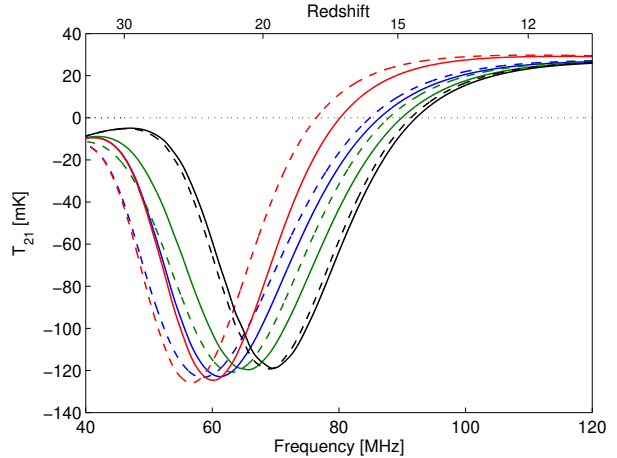


**Figure 1.** Global spectrum of the redshifted 21-cm brightness temperature with (solid) and without (dashed)  $v_{bc}$ , for the cases of no H<sub>2</sub> cooling (black), strong (green) and weak (blue) LW feedback and pure H<sub>2</sub> cooling without the negative feedback (red). Note that the red dashed line is the previously standard case for small halos.

## 2 GLOBAL HISTORY

The global spectrum of the redshifted 21-cm signal, and in particular the deep absorption feature expected to be observed at  $\sim 70$  MHz is a main target of some of the next generation experiments, such as the Large-aperture Experiment to detect the Dark Ages (LEDA) (Greenhill & Bernardi 2011). The exact shape and the central frequency of this feature both depend on the details of the evolution history of the Universe and in particular on the intensity and relative timing of the X-ray, LW and Ly $\alpha$  radiative backgrounds emitted by the first stars (see Figure 1 and Table 1).

Both the LW feedback (Fialkov et al. 2013) and relative velocities (Fialkov et al. 2011) delay star formation, which affects all the milestones of the global evolution of the Universe. For instance, the redshift of the heating transition, i.e., the moment when the gas heats up to the temperature of the CMB, is delayed by up to 17% in  $1+z$  when  $v_{bc}$  and the feedback are applied (Fialkov et al. 2013). To highlight the effect of the feedback on the important milestones of the high-redshift evolution history of the Universe (accounting also for  $v_{bc}$ ), we list here the redshifts of the Ly $\alpha$  transition  $z_{Ly\alpha}$  (defined as when the coupling of the spin temperature to the gas temperature becomes significant, specifically when the mean Ly $\alpha$  intensity equals the thermalization rate from Madau et al. (1997)), the heating transition  $z_h$  (when the mean gas temperature equals that of the CMB), and the epoch when LW feedback becomes significant  $z_{LW}$  (which is when the LW intensity equals  $J_{21} = 0.1$  in units of  $10^{-21} \text{ erg s}^{-1} \text{ cm}^{-2} \text{ Hz}^{-1} \text{ sr}^{-1}$ ). Our computational method allows us to study the relative timing between these transitions, which is considered highly uncertain in the literature (Pritchard & Loeb 2012). We find that (for our choice of model parameters) first to happen is the Ly $\alpha$  transition. The characteristic redshifts are  $1+z_{Ly\alpha} = 26.8$  in the case of H<sub>2</sub> cooling without the negative feedback,  $1+z_{Ly\alpha} = 26.5$  and  $24.6$  in the case of weak and strong LW feedback respectively, and  $1+z_{Ly\alpha} = 22.4$  in the case of no H<sub>2</sub> cooling. The LW feedback becomes important at

Feedback, $v_{bc}$	$\frac{dT_{21}}{d\nu}_{\max,1}$ $\left[\frac{\text{mK}}{\text{MHz}}\right]$	$\nu_{\max,1}$ [MHz] ( $z$ )	$T_{21,\min}$ [mK]	$\nu_{\min}$ [MHz] ( $z$ )	$\frac{dT_{21}}{d\nu}_{\max,2}$ $\left[\frac{\text{mK}}{\text{MHz}}\right]$	$\nu_{\max,2}$ [MHz] ( $z$ )
None, no $v_{bc}$	-11.6	48.5 (28.4)	-125.9	56.7 (24.2)	9.0	64.6 (21.1)
None, $v_{bc}$	-11.3	53.0 (26.0)	-124.7	60.1 (22.8)	8.7	68.2 (20.0)
Weak, no $v_{bc}$	-10.3	48.4 (28.5)	-123.2	58.5 (23.4)	6.5	69.9 (19.4)
Weak, $v_{bc}$	-10.5	53.0 (26.0)	-122.9	61.2 (22.3)	6.9	70.9 (19.2)
Strong, no $v_{bc}$	-8.6	53.1 (25.9)	-120.8	63.2 (21.6)	6.9	73.7 (18.4)
Strong, $v_{bc}$	-8.6	55.9 (24.5)	-119.6	65.7 (20.7)	6.9	74.7 (18.1)
No $H_2$ , no $v_{bc}$	-9.8	60.3 (22.7)	-119.3	69.2 (19.7)	7.6	78.3 (17.3)
No $H_2$	-9.7	62.8 (21.7)	-119.0	69.6 (19.5)	7.5	78.6 (17.2)

**Table 1.** Characteristics of the absorption trough in the global spectrum of the redshifted 21-cm signal, shown in Figure 1. Columns from left to right: the steepest negative slope of the spectrum; corresponding frequency (redshift); the minimum value of the brightness temperature; corresponding frequency (redshift); the steepest positive slope; corresponding frequency (redshift).

intermediate redshifts of  $1 + z_{LW} = 23.6$  for the strong feedback and  $1 + z_{LW} = 19.2$  for the weak feedback<sup>1</sup>. Finally, at lower redshifts the X-ray background heats the gas, with the transition at  $1 + z_h = 18.2, 16.9, 16.3,$  and  $15.9$  for  $H_2$  cooling without feedback, weak and strong feedbacks and no  $H_2$  cooling, respectively.

Naturally, the delayed star formation affects our predictions for the expected global spectrum of the 21-cm signal from high redshifts by blue-shifting the absorption trough. As we see from Figure 1, the general shape of the global spectrum varies only mildly as we change the strength of the feedback (or turn off  $v_{bc}$ ). For the most realistic cases (i.e., weak or strong feedback, including  $v_{bc}$ ), the spectrum reaches its minimum temperature of  $T_{21} = -121 \pm 2$  mK at  $\nu_{\min} = 63 \pm 2$  MHz (compare a shift of  $\Delta\nu \sim -2.5$  MHz if  $v_{bc}$  is turned off, and  $\Delta\nu \sim 6$  MHz if stars cannot form via  $H_2$  cooling; see Table 1).

The foreground galactic emission, which is the main noise component after the terrestrial interference is removed, is expected to be fairly smooth. Therefore it is easier to detect the signal if it changes fast with frequency. There are two characteristic frequencies for which the global 21-cm spectrum changes fast: the strongest change is at the low-frequency-end of the spectrum (high redshifts), at  $\nu_{\max,1} = 54.5 \pm 1.5$  MHz (for the most realistic cases) where the slope reaches  $|dT_{21}/d\nu| = 9.6 \pm 1.1$  mK/MHz; whereas the second strongest change happens at higher frequencies (low redshifts), at  $\nu_{\max,2} = 72.8 \pm 1.9$  MHz, where the slope is  $|dT_{21}/d\nu| \sim 6.9$  mK/MHz. Clearly, while the shape of the spectrum does not vary much with feedback (at least at fixed X-ray and Ly $\alpha$  efficiencies, as in this work), the frequencies  $\nu_{\min}$ ,  $\nu_{\max,1}$ , and  $\nu_{\max,2}$  substantially depend on the feedback strength (and  $v_{bc}$ ). Thus, measuring them may help us constrain the actual strength of the LW feedback in Nature.

### 3 EVOLUTION OF FLUCTUATIONS

The power spectrum of  $T_{21}$  may be easier to observe on top of the smooth foregrounds than the global spectrum, and it contains more information than the single curve. As we demonstrate further, the shape of the 21-cm power spectrum

evolves with redshift in a non-trivial way and has the power to constrain high- $z$  astrophysical processes.

Interestingly, we find that the heating fluctuations in the 21-cm signal are mostly decoupled from the Ly $\alpha$  fluctuations<sup>2</sup>. To illustrate this phenomenon we show in Figure 2 the redshift evolution of the 21-cm signal at the BAO scale (125 Mpc) and the peak-to-trough signal of BAOs in the brightness temperature. As in the case of the global signal, the shape of the curve is determined by the interplay between X-rays and Ly $\alpha$ , while the main role of the LW feedback (and  $v_{bc}$ ) is to delay the evolution and enhance large-scale fluctuations (in qualitative agreement with Visbal et al. (2012) and Fialkov et al. (2013)). The signal has two clear peaks: one at high redshifts (e.g.,  $z \sim 25$  in the case of strong feedback) which is sourced by fluctuations in the Ly $\alpha$  background, and the other at lower redshifts due to the fluctuations in the temperature of the gas ( $z \sim 18$  for the strong feedback). The exact values of the extremes of the signal and their corresponding redshifts for all of the discussed cases are listed in Table 2. The clear separation between these two domains means that the two regimes are disentangled, and that the onset of Ly $\alpha$  fluctuations and of the heating era can be measured separately. This would be a very powerful tool to explore astrophysical processes at high redshifts, such as the emissivity of the first galaxies in UV and X-rays, the halo masses that contribute to star formation at each redshift and the role of the negative feedback. Naturally, the spacing between the peaks would change if we were to alter our model parameters.

As was recently shown, heating fluctuations in the 21-cm power spectrum from high redshifts ( $z \sim 20$ ) are expected to be strong enough to be detectable even with present-day technology (Visbal et al. 2012). Here we demonstrate (Figures 2 and 3 and Table 3) that the fluctuations seeded by the inhomogeneous Ly $\alpha$  background are probably a bit too weak to be observed with an MWA/LOFAR-like telescope, but are expected to be strong enough to be detected by the next-generation SKA experiment. In other words, SKA should have enough sensitivity to detect the

<sup>1</sup> Note that this transition is not relevant for our two limiting cases of  $H_2$  cooling without feedback and of no  $H_2$  cooling.

<sup>2</sup> Pritchard & Furlanetto (2007) argued that Ly $\alpha$  photons from X-ray ionization are significant, but they appear to have overestimated the X-ray intensity relative to Ly $\alpha$  due to normalization errors. We find that  $\sim 100$  times higher X-ray intensity is needed to generate a significant Ly $\alpha$  contribution from X-rays.

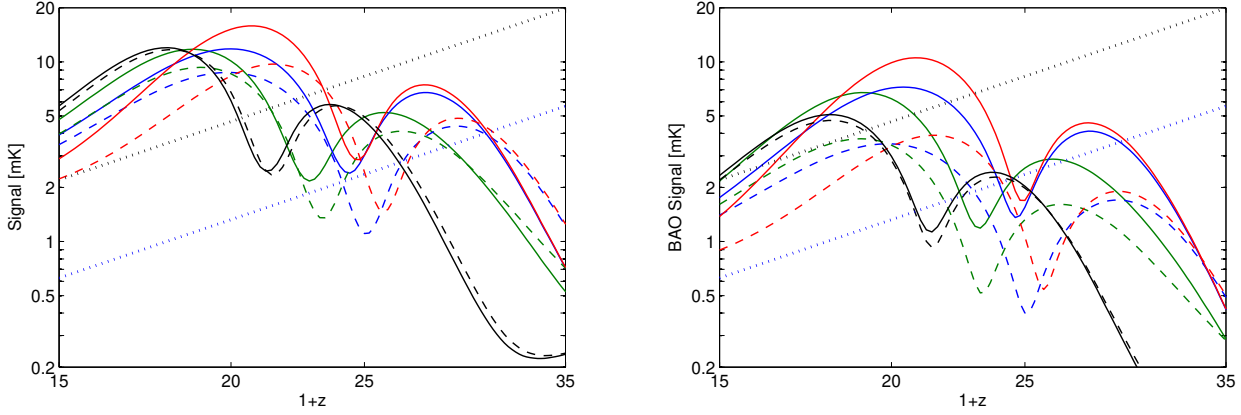


**Figure 2.** Left: amplitude of the 21-cm brightness temperature at 125 Mpc, the BAO scale. Right: peak-to-trough amplitude in BAOs, which we define to be the height of the BAO peak at  $2\pi/k = 125$  Mpc minus the depth of the trough at  $2\pi/k = 90$  Mpc (each feature measured with respect to a smoothed power spectrum with the BAOs removed). The two panels show the signal with (solid) and without (dashed)  $v_{bc}$  for no  $H_2$  cooling (black), strong (green) and weak (blue) feedback and for no feedback (red). We also show the sensitivity curves for SKA (blue dotted) and MWA/LOFAR-like (black dotted) experiments; the latter refers to an instrument with the same collecting area as MWA or LOFAR, and the former to the planned SKA, where to both we have applied an estimated degradation factor due to foreground removal (see McQuinn et al. (2006) and Visbal et al. (2012) for details).

Feedback, $v_{bc}$	$S_{\max,2}$ [mK]	$z$	$S_{\max,1}$ [mK]	$z$	$S_{\text{BAO,max},2}$ [mK]	$z$	$S_{\text{BAO,max},1}$ [mK]	$z$
None, no $v_{bc}$	9.7	19.6	4.9	27.4	3.9	19.6	1.9	27.4
None	15.8	18.8	7.5	25.6	10.5	18.8	4.6	25.8
Weak, no $v_{bc}$	8.9	18.0	4.4	27.2	3.5	17.9	1.7	27.2
Weak	12.1	18.1	6.7	25.8	7.2	18.4	4.1	25.8
Strong, no $v_{bc}$	9.5	17.0	4.1	24.6	3.7	17.0	1.6	24.6
Strong	12.0	16.8	5.2	23.8	6.9	17.1	2.9	24.2
No $H_2$ , no $v_{bc}$	12.0	16.2	5.7	21.8	4.9	16.2	2.3	21.8
No $H_2$	12.4	16.0	5.8	21.6	5.3	16.1	2.4	21.6

**Table 2.** The maximal values of the signal in  $T_{21}$  and in BAO together with the corresponding redshifts during the X-ray heating era (low- $z$ ) and the  $\text{Ly}\alpha$  coupling era (high- $z$ ). The Table summarizes the results from Figure 2.

Feedback, $v_{bc}$	$S/N_{\max,1}^{\text{MWA/LOFAR}}$	$z_1$	$S/N_{\max,2}^{\text{SKA}}$	$z_2$
None, no $v_{bc}$	2.2	19.6	1.7	27.6
None	3.4	19.0	2.6	26.2
Weak, no $v_{bc}$	2.5	17.6	1.6	27.5
Weak	3.0	17.7	2.3	26.2
Strong, no $v_{bc}$	3.0	17.1	1.9	25.0
Strong	3.5	16.8	2.3	24.2
No $H_2$ , no $v_{bc}$	4.1	16.5	3.2	22.6
No $H_2$	4.3	16.4	3.3	22.2

**Table 3.** Maximal values of the signal to noise from Figure 3.  $S/N_{\max,1}^{\text{MWA/LOFAR}}$  is the maximal S/N for an experiment like MWA or LOFAR for detection of heating fluctuations (low- $z$ ), while  $S/N_{\max,2}^{\text{SKA}}$  is the maximal signal to noise for detection of fluctuations from  $\text{Ly}\alpha$  coupling by the SKA.

complete early history of the 21-cm fluctuations, for any scenario of the LW feedback.

The shape of the power spectrum (Figure 3 right panel) depends on the nature of the fluctuations (either from the heating era or from the era of  $\text{Ly}\alpha$  coupling) and on the type of the feedback. The effect of the LW feedback and of  $v_{bc}$  on heating fluctuations (solid lines, right panel of Figure 3) was

discussed in detail in Fialkov et al. (2013) and Visbal et al. (2012). Here we complete the picture by including the effect of the  $\text{Ly}\alpha$  coupling (dashed lines, right panel of Figure 3). In fact, the strength of the feedback determines whether or not the LW transition happens during the heating era or the epoch of  $\text{Ly}\alpha$  coupling, which decides the character of the large-scale fluctuations. For instance, if the feedback is weak, it becomes relevant only at low redshifts, and affects mainly the X-ray heating, while only having a minor effect on the  $\text{Ly}\alpha$  fluctuations. On the other hand, if the feedback is strong, then the LW radiation begins early on to suppress the low-mass halos that are sensitive to the effect of  $v_{bc}$ , so the BAOs are substantially suppressed even during the  $\text{Ly}\alpha$  fluctuations. In any case, though, the LW feedback changes quite gradually with redshift Fialkov et al. (2013).

Clearly, the nature of the source of the fluctuations plays a significant role in shaping the power spectrum. In particular, the power spectrum from the era of  $\text{Ly}\alpha$  coupling is flat on scales smaller than  $\sim 100$  Mpc, which is of order the effective horizon for the  $\text{Ly}\alpha$  photons, within which the fluctuations are expected to be suppressed. In the X-ray case, a larger fraction of the flux is absorbed close to the source, and so the power spectrum is much steeper. We note that recently Mesinger et al. (2013) studied a model

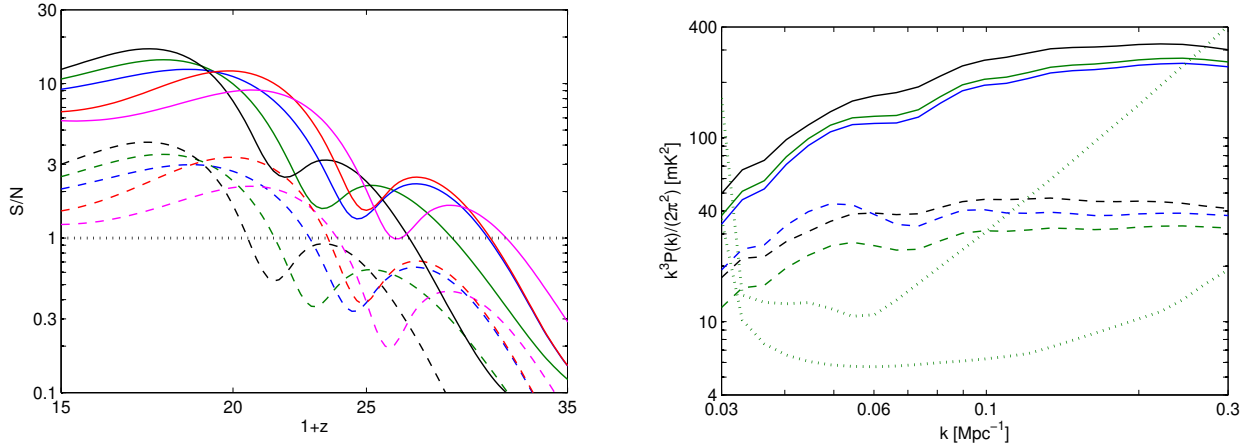


**Figure 3.** **Left:** Maximal S/N of the redshifted 21-cm signal at a single wavenumber  $k$  in the range  $k = 0.03 - 0.3 \text{ Mpc}^{-1}$ , where the signal is normalized by the noise of the SKA (solid lines) or by the noise of an MWA/LOFAR-like experiment (dashed lines). The colors refer to no feedback (red), weak (blue) and strong (green) LW feedbacks or no  $H_2$  cooling (black), and all cases include  $v_{bc}$ . We also show the previously standard case for small halos, which neglected both  $v_{bc}$  and feedback (magenta curves). **Right:** Power spectrum for the realistic cases (with  $v_{bc}$ ) of strong (green) and weak (blue) feedbacks and no  $H_2$  cooling (black) calculated at the corresponding redshifts of the low- $z$  (solid) and the high- $z$  (dashed) peaks in the S/N from the left panel of this Figure. The redshifts are 17.6 and 26.2 for the weak feedback, 16.8 and 24.2 for the strong feedback, and 16.4 and 22.4 for the no  $H_2$  case. The upper dotted line correspond to the sensitivity curve of MWA/LoFAR at  $z = 16.8$  (low- $z$  S/N peak of the strong feedback case), while the lower dotted line corresponds to the sensitivity of SKA at  $z = 24.2$ , the redshift of the high- $z$  S/N peak in the strong feedback case. Analogous sensitivity curves for the weak feedback case would be higher by a factor of about 1.3 (MWA/LoFAR) or 1.5 (SKA); for no  $H_2$  cooling case the curves would be lower by 1.1 (MWA/LoFAR) or 1.5 (SKA).

similar to our no  $H_2$ , no  $v_{bc}$  case; in this extreme case of no star formation from  $H_2$  cooling, we find that adding  $v_{bc}$  still shifts the key 21-cm features by up to a few percent.

To summarize, we have shown that the prospects for observing the complete early history of the Universe via fluctuations in the 21-cm signal are very promising. Future 21-cm observations are expected to constrain the formation history and properties of stars and galaxies at high redshifts. The effect of fluctuations in the Ly $\alpha$  and X-ray backgrounds on the 21-cm power spectrum are likely to be mostly decoupled in time and can be studied separately. Also, the LW feedback plays a unique role by delaying star formation and thus can be constrained independently.

#### 4 ACKNOWLEDGMENTS

This work was supported by Israel Science Foundation grant 823/09. A.F. was also supported by European Research Council grant 203247.

#### REFERENCES

- Barkana, R., & Loeb, A. 2001, *Phys. Rep.*, 349, 125  
 Barkana R., Loeb A., 2004, *ApJ*, 609, 474  
 Barkana R., Loeb A., 2005, *ApJ*, 626, 1  
 Bowman J. D., Morales M. F., Hewitt J. N., 2009, *ApJ*, 695, 183  
 Carilli, C. L., Furlanetto, S., Briggs, F., Jarvis, M., Rawlings, S., Falcke, H., 2004, *NewAR*, 48, 11-12  
 Dalal, N., Pen, U.-L., Seljak, U., 2010, *JCAP*, 11, 7  
 Fialkov A., Barkana R., Tseliakhovich D., Hirata C. M. 2012, *MNRAS*, 424, 1335

- Fialkov A., Barkana R., Visbal, E., Tseliakhovich D., Hirata C. M., 2013, *MNRAS*, in press  
 Field, G. B., 1958, *Proc. Institute Radio Engineers*, 46, 240  
 Greenhill, L. J., Bernardi, G., 2012, arXiv:1201.1200  
 Greif, T., White, S., Klessen, R., & Springel, V., 2011, *ApJ*, 736, 147  
 Haiman, Z., Rees, M. J., Loeb, A., 1997, *ApJ*, 484, 985  
 Harker, G., 2010, *MNRAS*, 405, 2492  
 Holzbauer L. N., Furlanetto S. R., 2012, *MNRAS*, 419, 718  
 Komatsu, E. et al., 2011, *ApJS*, 192, 18  
 Machacek, M. E., Bryan, G. L., Abel, T., 2001, *ApJ*, 548, 509  
 Madau, P., Meiksin, A., Rees, M. J., 1997, *ApJ*, 475, 429  
 McQuinn, M., Zahn, O., Zaldarriaga, M., Hernquist, L., Furlanetto, S. R., 2006, *ApJ*, 653, 815  
 Mesinger, A., Furlanetto, S., Cen, R., 2011, *MNRAS*, 411  
 Mesinger, A., Ferrara, A., & Spiegel, D. S., 2013, *MNRAS*, 431, 621  
 Naoz, S., Barkana, R., 2008, *MNRAS*, 385, L63  
 Naoz, S., Yoshida, N., Gnedin, N. Y., 2013, *ApJ*, 763, 27  
 O’Shea, B. W., Norman, M. L., *ApJ*, 673, 14, 2008  
 Pritchard, J. R., Furlanetto, S., 2007, *MNRAS*, 376, 1680  
 Pritchard, J. R., Loeb, A., 2012, *Rep. Prog. Phys.*, 75, 35  
 Stacy A., Bromm V., Loeb A., 2011, *ApJ*, 730, 1  
 Tegmark M., Silk J., Rees M. J., Blanchard A., Abel T., Palla F., 1997, *ApJ*, 474, 1  
 Tseliakhovich D., Hirata C. M., 2010, *PRD*, 82, 083520  
 Tseliakhovich D., Barkana R., Hirata C. M. 2011, *MNRAS*, 418, 906  
 Visbal, E., Barkana, R., Fialkov, A., Tseliakhovich, D., Hirata, C. M., 2012, *Nature*, 487, 70  
 Wise, J. H., Abel, T., 2007, *ApJ*, 671, 1559  
 Wouthuysen, S. A., 1952, *AJ*, 57, 31